International Journal of Clinical Oncology
https://doi.org/10.1007/s10147-024-02507-1

ORIGINAL ARTICLE

Progressive changes in the protein expression profile of alveolar septa in early-stage lung adenocarcinoma

Toru Kimura[1,2] · Takashi Akazawa[3] · Yu Mizote[3] · Harumi Nakamura[4] · Miki Sakaue[1] · Tomohiro Maniwa[1] · Yasushi Shintani[2] · Keiichiro Honma[5] · Hideaki Tahara[3,6] · Jiro Okami[1]

Received: 8 November 2023 / Accepted: 6 March 2024

Abstract

Background Adenocarcinomas show a stepwise progression from atypical adenomatous hyperplasia (AAH) through adenocarcinoma in situ (AIS) to invasive adenocarcinoma (IA). Immunoglobulin superfamily containing leucine-rich repeat (ISLR) is a marker of tumor-restraining cancer-associated fibroblasts (CAFs), which are distinct from conventional, strongly α-smooth muscle actin (αSMA)-positive CAFs. Fibroblast activation protein (FAP) has been focused on as a potential therapeutic and diagnostic target of CAFs.

Methods We investigated the changes in protein expression during adenocarcinoma progression in the pre-existing alveolar septa by assessing ISLR, αSMA, and FAP expression in normal lung, AAH, AIS, and IA. Fourteen AAH, seventeen AIS, and twenty IA lesions were identified and randomly sampled. Immunohistochemical analysis was performed to evaluate cancer-associated changes and FAP expression in the pre-existing alveolar structures.

Results Normal alveolar septa expressed ISLR. The ISLR level in the alveolar septa decreased in AAH and AIS tissues when compared with that in normal lung tissue. The αSMA-positive area gradually increased from the adjacent lung tissue (13.3% ± 15%) to AIS (87.7% ± 14%), through AAH (70.2% ± 21%). Moreover, the FAP-positive area gradually increased from AAH (1.69% ± 1.4%) to IA (11.8% ± 7.1%), through AIS (6.11% ± 5.3%). Protein expression changes are a feature of CAFs in the pre-existing alveolar septa that begin in AAH. These changes gradually progressed from AAH to IA through AIS.

Conclusions FAP-positive fibroblasts may contribute to tumor stroma formation in early-stage lung adenocarcinoma, and this could influence the development of therapeutic strategies targeting FAP-positive CAFs for disrupting extracellular matrix formation.

Keywords Cancer-associated fibroblast · Fibroblast-activation protein · Lepidic growth · Lung adenocarcinoma · Tumor stroma

✉ Toru Kimura
kimura@thoracic.med.osaka-u.ac.jp

[1] Department of General Thoracic Surgery, Osaka International Cancer Institute, 3-1-69, Otemae, Chuo-Ku, Osaka 541-8567, Japan

[2] Department of General Thoracic Surgery, Osaka University Graduate School of Medicine, 2-2-L5, Yamadaoka, , Suita 565-0871, Japan

[3] Department of Cancer Drug Discovery and Development, Research Center, Osaka International Cancer Institute, 3-1-69, Otemae, Chuo-Ku, Osaka 541-8567, Japan

[4] Laboratory of Genomic Pathology, Osaka International Cancer Institute, 3-1-69, Otemae, Chuo-Ku, Osaka 541-8567, Japan

[5] Department of Pathology, Osaka International Cancer Institute, 3-1-69, Otemae, Chuo-Ku, Osaka 541-8567, Japan

[6] Project Division of Cancer Biomolecular Therapy, Institute of Medical Science, The University of Tokyo, 4-6-1 Shirokanedai, Minato-Ku, Tokyo 108-8639, Japan

Published online: 11 April 2024

Introduction

Adenocarcinoma is the most common type of lung cancer worldwide [1]. Among the histological subtypes of invasive non-mucinous adenocarcinoma, it often presents as mixed histology, which includes a combination of lepidic, acinar, papillary, micropapillary, or solid growth patterns [2]. Several peripheral-type adenocarcinomas exhibit a lepidic growth area during the early phase and show a stepwise progression from atypical adenomatous hyperplasia (AAH) to adenocarcinoma in situ (AIS) and invasive adenocarcinoma (IA) including minimally invasive adenocarcinoma [3]. The foci of active fibroblastic proliferation and thickening of the alveolar septa are considered IA indicators [3, 4]. However, the time at which the changes in protein expression begin to occur in the pre-existing alveolar septa of normal lung tissues, AAH, and AIS remains unclear.

Cancer-associated fibroblasts (CAFs) constitute a highly abundant stromal cell type in solid cancers, comprising a microenvironment that includes secreted proteins and extracellular matrix (ECM) components [5]. Although α-smooth muscle actin (αSMA) was previously considered an ideal biomarker for activated fibroblasts, the recent proposal of several other biomarkers for activated fibroblasts in various cancer kinds, including non-small cell lung cancer, clearly illustrates the heterogeneous nature of CAFs [6]. The immunoglobulin superfamily containing leucine-rich repeat (ISLR), also known as Meflin, is a glycosylphosphatidylinositol-anchored protein encoded by an immunoglobulin superfamily containing a leucine-rich repeat gene. It has been reported as a potential marker for mesenchymal stromal cells [7]. ISLR is a marker for tumor-restraining CAFs [8, 9], and its mRNA expression in CAFs is weakly positive or negative for αSMA expression and is distinct from that of conventional strongly αSMA-positive CAFs in lung adenocarcinoma [10]. However, ISLR protein expression and correlation with αSMA protein expression in the alveolar septa of normal lung tissue, AAH, and AIS are not well known.

Fibroblast activation protein (FAP) is a cell surface serine protease expressed by CAFs but not by the actual tumor cells in most solid tumors; therefore, it may serve as a marker for CAFs [11]. The gene expression profile of FAP-positive fibroblasts is enriched in inflammatory genes, matrix components, matrix remodeling enzymes, and epithelial cell growth factors [12, 13]. Recently, activated fibroblasts that express FAP, rather than those that express αSMA, have been shown to play a role in ECM formation [12]. FAP-positive fibroblasts are selectively induced in areas of ongoing tissue remodeling, including wound healing [14], fibrosis [15], and solid tumor microenvironment [16]. While FAP is known to be overexpressed in breast, colorectal, pancreatic, bladder, ovarian, and other cancers, the impact of FAP expression on disease prognosis varies from study to study [17]. Previous studies on lung adenocarcinoma have identified FAP expression in tumor stroma as a marker of poor prognosis [18–21]. Furthermore, developing small molecules that target FAP to act as tracers in positron emission tomography and radionuclide therapy has sparked considerable interest in oncological research, including lung cancer research [22–24]. FAP-positive fibroblasts serve as therapeutic targets for cellular immunotherapy in cardiac fibrosis and cancer to reduce fibrotic reactions and ECM formation, respectively [25–27]. However, FAP expression and its temporal transition in AAH and early-phase adenocarcinoma, in which the pre-existing alveolar septa start thickening and undergo fibrotic changes, are not well researched.

We hypothesized that the changes in the protein expression in the alveolar septa would begin during AAH and that alveolar septa thickening in early-phase adenocarcinoma could be due to stromal formation by FAP-expressing cells. To verify this hypothesis, we examined ISLR and αSMA protein expression levels to identify the alterations in their expression patterns. Moreover, we investigated FAP expression in the pre-existing alveolar structures in AAH and AIS and the lepidic growth areas in IA.

Methods

Patients

We searched our pathology database from January 2018 to December 2019 using retrieval words, such as "atypical adenomatous hyperplasia" or "AAH." During this period, 554 patients had undergone surgical resection for lung cancer at Osaka International Cancer Institute. Of these, 13 patients yielded 14 AAH lesions. Seven patients underwent surgical resections for other lesions—3 patients exhibited AIS lesions, 2 showed IA lesions, 1 exhibited metastatic pulmonary nodule lesions, and 1 exhibited inflammatory pulmonary nodule lesions. A total of 17 AIS and 20 IA lesions, including a lepidic component, were randomly selected from the surgical resections during the study period. To assess the stepwise progression of lung adenocarcinoma, particularly within the pre-existing alveolar structure, we specifically selected IA lesions that included a lepidic component. These lesions comprised of seven minimally invasive adenocarcinomas, nine lepidic-predominant IAs, one papillary-predominant IA, and three acinar-predominant IAs.

Histologic evaluation

All resected tissue samples were evaluated clinically using a light microscope with a standard 22-mm eyepiece by certified pathologists from our institute. Pathological diagnosis of cancer cell invasiveness, which is assessed based on the destruction of the elastic fiber framework, was clinically evaluated using Elastica van Gieson staining at our institute.

Multiplex immunofluorescence (mIF) staining

mIF staining was performed using an Opal 4-Color Automation IHC kit (#NEL820001KT; Akoya Biosciences, Marlborough, MA, USA) on a Leica BOND RX automated immunostainer (Leica Microsystems Ltd., Milton Keynes, UK) according to the manufacturer's instructions. Briefly, all tissue sections were baked at 60 °C for 30 min, soaked in BOND Dewax Solution at 72 °C, and then rehydrated in ethanol for deparaffinization. Next, the tissue sections were subjected to antigen retrieval and blocking using BOND Epitope Retrieval Solution 1 (citrate-based pH 6 epitope-retrieval solution) and Antibody diluent/Block solution (Akoya Biosciences), respectively. Thereafter, they were sequentially treated with the primary antibody Opal Polymer HRP Ms + Rb and each Opal fluorophore (Opal 520, 570, or 690), and the antibody was subsequently stripped by baking. After three repetitions of the above processes, from blocking to antigen stripping, the sections were counterstained with spectral 4′,6-diamidino-2-phenylindole. The following combinations of the antibody (dilution) and Opal reagent were used in the experiment: E-cadherin (1:500, clone EP700Y, #ab40772; Abcam, Cambridge, UK) for Opal 520/690, ISLR (1:200, rabbit polyclonal, #ab232986; Abcam) for Opal 570, and αSMA (1:100, clone 1A4, #M0851; Agilent Technologies, Santa Clara, CA, USA) for Opal 690. The mIF images were acquired using the Olympus Slide Scanner VS200 (Olympus, Tokyo, Japan).

To measure the area positive for ISLR or αSMA in the stromal area, we used the ImageJ software (ver.1.53t; https://imagej.nih.gov/ij/; NIH, Bethesda, MD, USA) to analyze the mIF-stained sections. Each lesion site and the adjacent lung field from the same section were trimmed and split into color channels. After determining the optimal and common thresholds, each image was converted into a binary image to identify the areas positive for ISLR or αSMA. The ratio of ISLR- or αSMA-positive areas in the stromal area was calculated using the following formula:

$$100 \times (\text{ISLR} - \text{ or } \alpha\text{SMA} - \text{positive area}) \Big/ \left[(\text{ISLR} - \text{positive area}) + (\alpha\text{SMA} - \text{positive area})\right].$$

Immunohistochemical staining

For immunohistochemical identification of FAP-positive cells after antigen retrieval, the tissue sections were stained with rabbit – antihuman FAP monoclonal IgG (1:245, 3 μg/mL, clone EPR20021, # ab207178; Abcam). For isotype control staining, the same concentration of rabbit IgG (#011–000-003; Jackson ImmunoResearch, West Grove, PA, USA) was used. For antigen retrieval corresponding to these antibodies, the sections were treated with 10 mM sodium citrate buffer containing 0.05% Tween for 20 min at 100 °C. The secondary antibody (goat – antirabbit IgG H and L [HRP polymer], #ab214880; Abcam) was detected using 3,3′-diaminobenzidine (DAB).

Immunohistochemical analysis

Two independent researchers evaluated FAP staining positivity. For FAP dichotomization in terms of expression, the sections with relatively low or no staining were considered "Low," and the rest were recorded as "High," as described previously [17]. For objective and quantitative evaluation of FAP staining, machine learning image analysis was performed using ZEISS ZEN3.2 (Carl Zeiss Microscopy, Oberkochen, Germany), as described previously [28]. Whole-slide images were exported in TIFF format (approximately 20,000 × 10,000 pixels), and approximately 10 characteristic structural parts (approximately 2000 × 2000 pixels) were extracted from each section. Using ZEISS ZEN Intellesis, machine learning was employed to recognize and sort lepidic components into FAP-positive and -negative areas based on the extracted TIFF images. The FAP-positive areas were analyzed using this module. The percentage of FAP-positive areas in the lepidic structure was calculated using the following equation:

$$100 \times (\text{FAP} - \text{positive area in lepidic component}) \Big/ \left[(\text{lepidic component}) + (\text{FAP} - \text{positive area in lepidic component})\right].$$

Immunoblotting

Normal lung tissues were surgically obtained from patients with lung cancer. These were floated in ice-cold RIPA lysis buffer containing Halt Protease Inhibitor Cocktail (Thermo Fisher Scientific, Waltham, MA, USA) and homogenized using a gentleMACS Dissociator (Miltenyi Biotec, Bergisch Gladbach, Germany). After centrifugation at 4000 × *g* for 5 min, the tissue lysates were collected, mixed with 4 × SDS-PAGE sample buffer (#B6104; Tokyo Chemical Industry, Tokyo, Japan) and 5% 2-mercaptoethanol, and boiled at 95 °C for 5 min to denature proteins. Some samples were

treated with PNGase F (#P0704; New England BioLabs, Ipswich, MA, USA) and incubated overnight at 37 °C to remove N-linked oligosaccharides. Each tissue lysate was loaded on 4–20% Mini-PROTEAN TGX Gels (#4561096; Bio-Rad Laboratories, Hercules, CA, USA) and separated using sodium dodecyl sulfate–polyacrylamide gel electrophoresis. The proteins in the gel were transferred to an Immobilon-P transfer membrane (#IPVH07850; Merck Millipore, Burlington, MA, USA). The membrane was first treated with a primary antibody, either anti-ISLR Abs (2 µg/mL, #ab232986; Abcam) or anti-β-actin mAb (1:10,000, clone6D1, #010-27841; FUJIFILM Wako, Osaka, Japan), and then with a secondary antibody, either HRP-conjugated antirabbit IgG Abs (1:10,000, #611-035-215; Jackson ImmunoResearch) or HRP-conjugated anti-mouse IgG Abs (1:2,000, #615-035-214; Jackson ImmunoResearch). Chemiluminescence was measured using a Clarity Western ECL Substrate (#1705060; Bio-Rad Laboratories) and detected using Luminograph (ATTO, Tokyo, Japan).

Statistical analysis

Associations across variables were analyzed using Fisher's exact and chi-square tests. As appropriate, statistical significance between paired groups was checked using Mann−Whitney U test or unpaired Student's *t* test. An one-way analysis of variance followed by a post hoc test was used for multiple-group comparisons. Statistical significance was considered when $p \leq 0.05$. Statistical analyses were conducted using GraphPad Prism 8 for Windows 64-bit, version 8.4.3 (GraphPad Software, San Diego, CA, USA) or EZR (Saitama Medical Center, Jichi Medical University, Saitama, Japan), which is a graphical user interface for R (R Foundation for Statistical Computing, Vienna, Austria) [29].

Results

The clinical features of all included patients, who had AAH/AIS/IA lesion samples, are presented in Table 1. Age, sex, smoking history, respiratory coexisting diseases, body mass index (BMI), and tumor location did not show any significant differences among the patients with lung nodules. None of the patients had any respiratory or systemic diseases that could be considered to have an impact on lung inflammation and fibrosis. Genetic testing was conducted on five patients of IA, all of which tested negative for epidermal growth factor receptor mutation.

First, we evaluated the alteration in protein expression in the alveolar septa in AAH, AIS, and IA lung tissue samples. Normal alveolar septa expressed ISLR (Fig. 1a–e). Immunoblotting confirmed that ISLR was expressed and usually *N*-glycosylated in the normal lung and that the antibodies were able to recognize both its native and glycosylated forms (Fig. 2). In the alveolar septa of AAH lesions, the expression of ISLR decreased, whereas that of αSMA increased (Fig. 1g–j). Furthermore, in the alveolar septa of AIS lesions, the protein expression of αSMA was evident, whereas that of ISLR was not (Fig. 1l–o). According to the histological findings based on HE staining, the pre-existing alveolar septa in the normal lung, AAH, and AIS were mainly composed of spindle-shaped cells and extracellular matrix (Fig. 1f, k, p). The quantitative evaluation of the αSMA area (%) in the adjacent lung tissue and the AAH, AIS, and IA lesions using ImageJ showed that the αSMA-positive area gradually increased from the adjacent lung tissue (13.3% ± 15%) through AAH lesion (70.2% ± 21%) to AIS lesion (87.7% ± 14%) (adjacent lung vs. AAH—$p < 0.0001$; adjacent lung vs. AIS—$p < 0.0001$; adjacent lung vs. IA—$p < 0.0001$; AAH vs. AIS—$p = 0.035$; AAH vs. IA—$p = 0.000157$) (Fig. 3). These findings indicate that the protein expression of ISLR, relative to αSMA, in the alveolar septa decreased in AAH and AIS lesion tissue when compared with that in normal lung tissue. In relative to ISLR expression, αSMA expression in the alveolar septa,

Table 1 Patient characteristics in an early-stage adenocarcinoma study

		AAH ($n=13$)	AIS ($n=17$)	IA ($n=20$)	p**
Age	(year)	67.4 ± 8.5*	69.3 ± 9.1*	68.6 ± 7.2*	0.82
Sex	Male	6	5	10	0.444
	Female	7	12	10	
Smoking	Never	5	11	9	0.393
	Ex	8	6	11	
Pack-year	< 20	8	13	12	0.523
	> 20	5	4	8	
BI		273 ± 380*	267 ± 462*	411 ± 533*	0.593
Respiratory disease coexistence	Asthma	2	1	3	0.206
	COPD	2	0	3	
	None	9	16	14	
Side	Right	8	11	10	0.761
	Left	5	6	9	
Lobe	Upper	8	7	9	0.774
	Middle	1	1	1	
	Lower	4	9	10	
BMI		23.4 ± 2.6	22.3 ± 2.7	23.2 ± 2.7	0.492

BI Brinkman Index, *COPD* chronic obstructive pulmonary disease, *AAH* atypical adenomatous hyperplasia, *AIS* adenocarcinoma in situ, *IA* invasive adenocarcinoma, *BMI* body mass index

*Age and BI data are reported as average ± SD

**Associations across variables were analyzed using Fisher's exact and chi-square tests

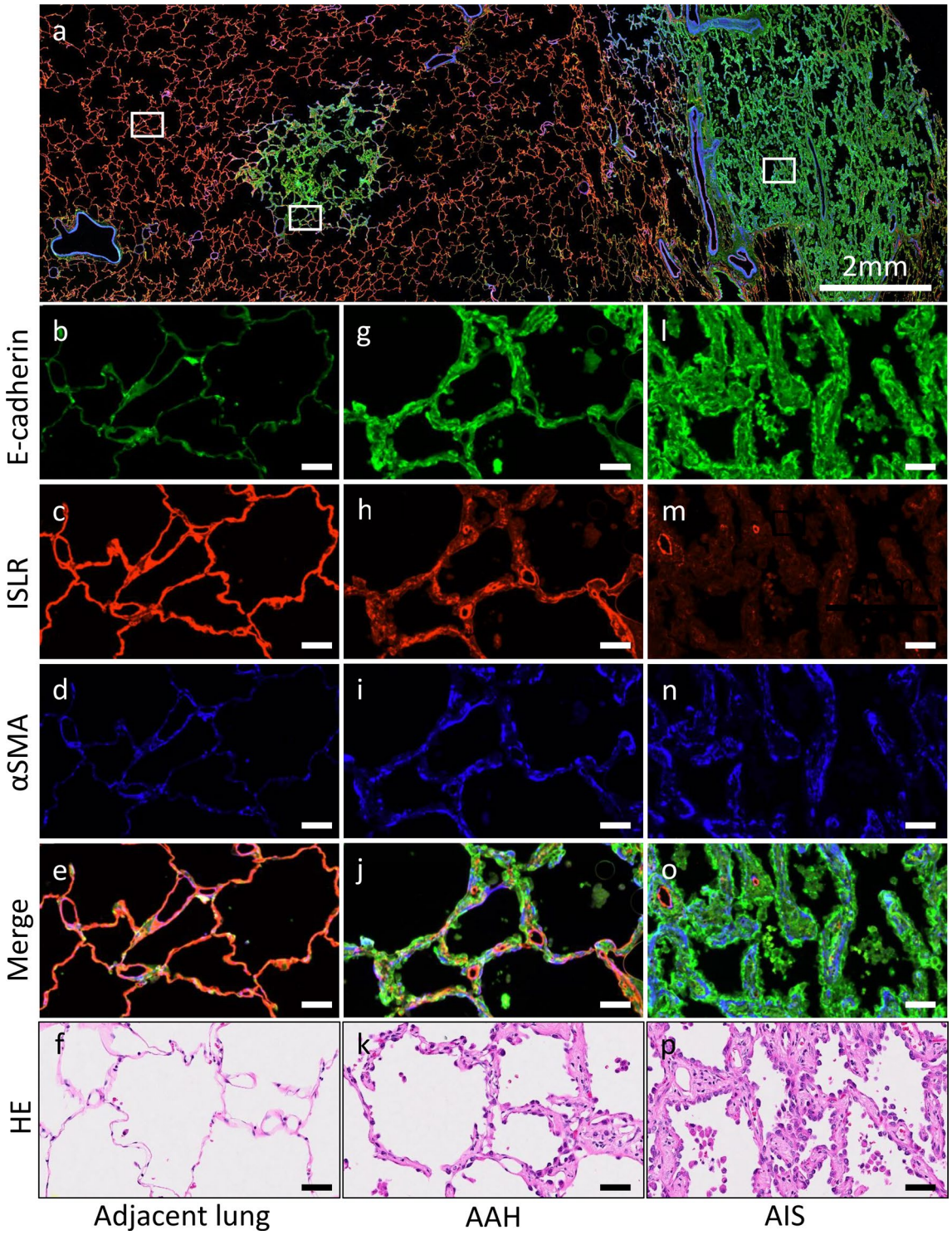

Fig. 1 Multiple immunofluorescences of tissue sections. Tissue sections derived from a patient with atypical adenomatous hyperplasia (AAH) and adenocarcinoma in situ (AIS) were stained for multiplex immunofluorescence using E-cadherin as an epithelial marker (green, **b/f/j**), immunoglobulin superfamily containing leucine-rich repeat (ISLR, red, **c/g/k**), and α-smooth muscle actin (αSMA, blue, **d/h/l**), followed by imaging using a multispectral imaging system (**a/e/i/m**). Representative images of normal lung tissue (left square in **a**, **b**–**f**) and AAH (middle square in **a**, **g**–**k**) and AIS (right square in **a**, **l**–**p**) lesions. The complete image of the HE-stained slide is available in the Online Resource

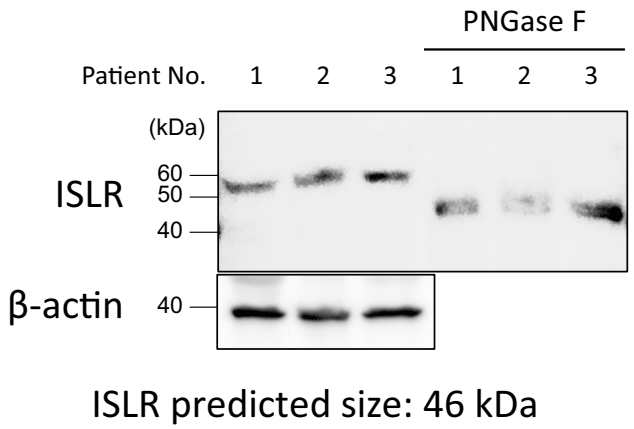

Fig. 2 Immunoblotting of immunoglobulin superfamily containing leucine-rich repeat (ISLR) in whole lung lysates and those treated with PNGase F for removing *N*-linked oligosaccharides. Uncropped images of immunoblotting are provided in the Online Resource

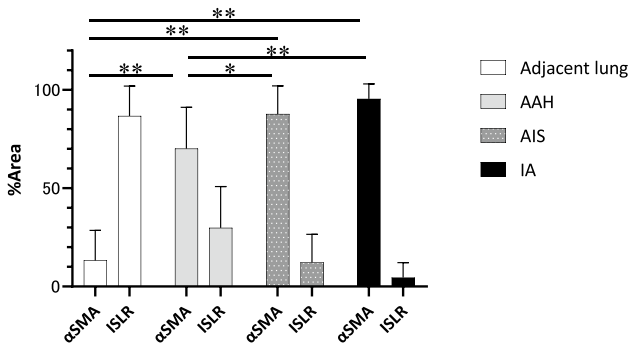

Fig. 3 Quantitative analysis of protein expression in the alveolar septa. Quantitative analysis of immunoglobulin superfamily containing leucine-rich repeat (ISLR) and α-smooth muscle actin (αSMA) expression in the alveolar septa. Quantitative analysis of ISLR and αSMA expression in the alveolar septa of adjacent lung tissue and atypical adenomatous hyperplasia (AAH), adenocarcinoma in situ (AIS), and invasive adenocarcinoma (IA) lesions (*$p<0.05$, **$p<0.005$). As appropriate, statistical significance between paired groups was checked using Mann−Whitney *U* test or unpaired Student's *t* test

a known feature of CAFs, was initiated even in AAH lesions and then increased in AIS.

Next, we evaluated the expression of FAP in the alveolar septa of AAH and AIS and the lepidic growth area of IA, where the protein expression was altered when compared with that in the normal lung (Fig. 4a–e). As shown in Table 2, the percentage of FAP-positive lesions among AIS and IA samples was significantly higher than that in AAH samples ($p=0.0042$ and $p<0.0001$, respectively). The evaluation of the percentage of FAP-positive area in AAH and AIS, as well as the lepidic growth area of IA using machine learning image analysis, showed that the FAP-positive area gradually increased from AAH (1.69% ± 1.4%) through AIS (6.11% ± 5.3%) to IA (11.8% ± 7.1%) (AAH vs. AIS, $p=0.0111$; AAH vs. IA, $p<0.0001$; AIS vs. IA, $p=0.0275$) (Fig. 4f).

Discussion

This study demonstrated the changes in ISLR and αSMA expression in the alveolar septa during AAH—a pre-cancerous lung lesion associated with atypical alveolar epithelial cells. αSMA is one of the well-known specific markers of spindle-shaped CAFs [11]. Although the alveolar structure in AAH is similar to that in normal lung tissue, mIF staining revealed a decrease in the expression of ISLR and an increase in the expression of αSMA in the alveolar septa. As a subset of CAFs, cells expressing *ISLR* mRNA have been reported to be weakly positive or negative for αSMA, and they are distinct from conventional strongly αSMA-positive CAFs [9]. The protein expression of ISLR has not been evaluated, especially in normal lung tissues. As there are no reports on ISLR expression in the normal lung parenchyma, we confirmed the protein expression of ISLR in the lung tissue using immunoblotting to rule out the nonspecific binding of the ISLR antibody to the lung parenchyma in mIF staining. Our results showed that ISLR protein expression in the interstitium of normal lung parenchyma was gradually replaced by αSMA protein expression in AAH and AIS lung tissues. To the best of our knowledge, this is the first study to clearly show that the protein expression of αSMA in alveolar septa begins in AAH, although this phenomenon has been known to occur in the stroma of various types of cancers [30]. Notably, the staining results suggested that even in AAH, which is not a cancerous lesion, stromal cells could be influenced by the "atypical" epithelial cells to transform transiently into the stroma of malignant lesions.

Next, we found that FAP expression in the alveolar septa gradually increased in the following order: AAH < AIS < IA (lepidic growth area). This result is consistent with the transcriptome sequencing data obtained from tissue samples of lung adenocarcinoma, AAH, and normal lung. The data showed that FAP expression in lung adenocarcinoma and AAH was higher as compared to normal lung [31]. This study is the first to demonstrate pathologically that FAP expression in pre-existing alveolar septa can be observed in some pre-cancerous lesions, such as AAH and AIS. In nononcologic lung diseases like idiopathic pulmonary fibrosis, it is well-known that FAP is upregulated in fibroblastic foci and fibrotic interstitium of the affected lung [32]. As activated fibroblasts, which express FAP instead of αSMA, are involved in ECM formation [12], FAP-expressing cells in pre-existing alveolar septa, influenced by neoplastic cells, may contribute to the fibrotic changes in pre-cancerous lesions and the lepidic

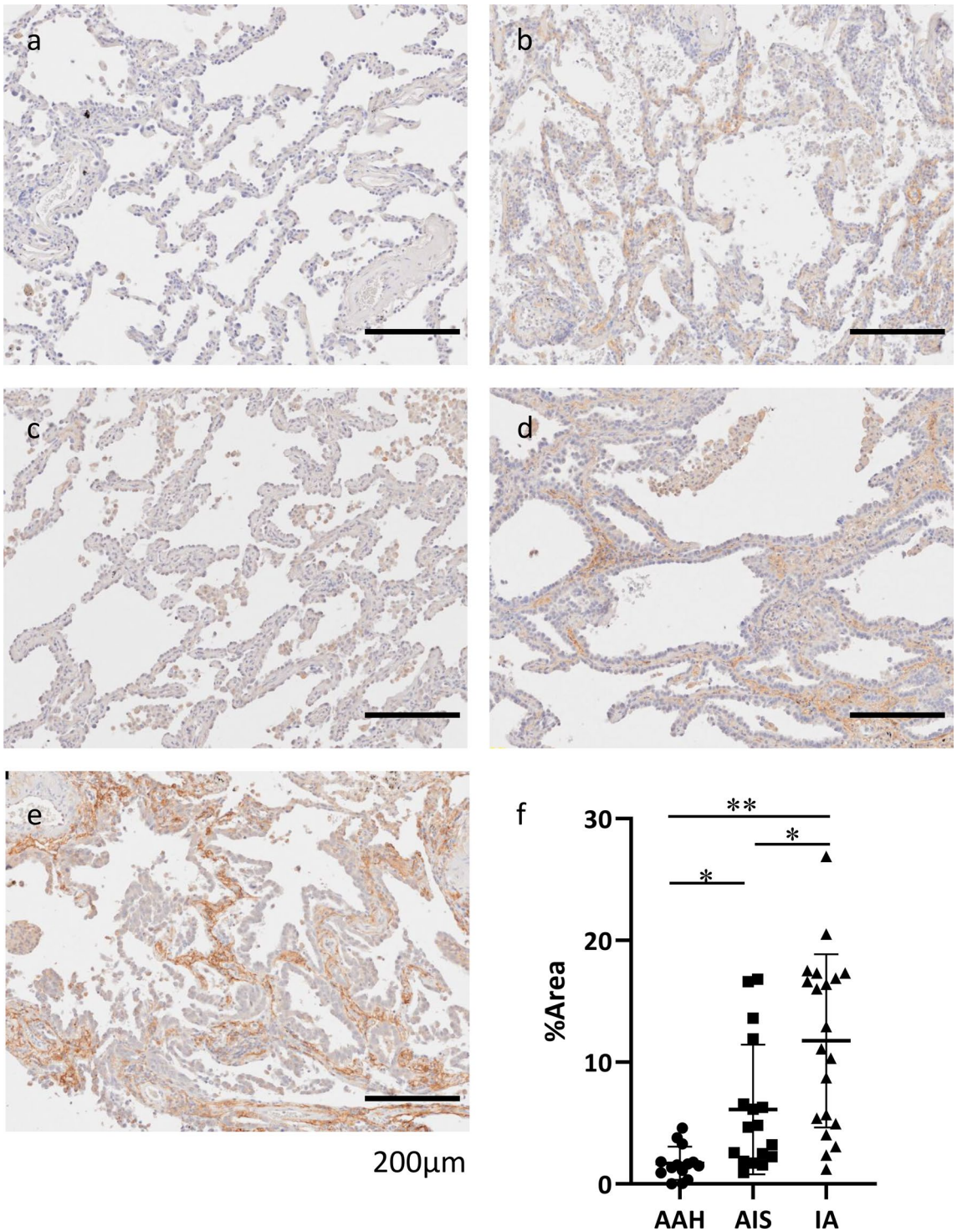

Fig. 4 Examples of fibroblast-activation protein expression observed using immunohistochemistry. Representatives of **a** FAP-negative and **b** FAP-positive atypical adenomatous hyperplasia (AAH); **c** FAP-negative and **d** FAP-positive adenocarcinoma in situ (AIS); and **e** FAP-positive lepidic growth area of invasive adenocarcinoma (IA). Percentage of FAP-positive areas in AAH ($n=14$), AIS ($n=17$), and lepidic growth area of IA ($n=20$) were obtained using machine learning image analysis; $^{*}p<0.05$, $^{**}p<0.001$ (**f**). As appropriate, statistical significance between paired groups was checked using Mann–Whitney *U* test or unpaired Student's *t* test

Table 2 Expression of fibroblast-activation protein (FAP) in lung adenocarcinoma

		AAH ($n=14$)	AIS ($n=17$)	IA ($n=20$)	P*
FAP	High	1 (7.1%)	12 (70.6%)	18 (90.0%)	<0.0001
	Low	13 (92.9%)	5 (29.4%)	2 (10.0%)	

AAH atypical adenomatous hyperplasia, *AIS* adenocarcinoma in situ, *IA* invasive adenocarcinoma

*Associations across variables were analyzed using Fisher's exact and chi-square tests

growth area of early-stage lung adenocarcinoma. FAP expression in the tumor stroma of lung adenocarcinoma has been reported as a marker of poor prognosis [18–21], and the proliferation of CAFs might indicate a very early phase of invasiveness in early-stage lung adenocarcinoma [33]. Considering the consistent findings in the literature regarding the effect of FAP on cell proliferation, migration, and invasion [17], it is possible that FAP-expressing cells in pre-existing alveolar septa in early-stage lung adenocarcinoma are involved, as the next step, in the development of an invasive phenotype.

With the recent development of positron emission tomography and radionuclide therapy that targets FAP in oncological research, including lung cancer [22–24], this imaging system may be available for the detection of early-stage lung cancers such as AIS, and minimally IA. Furthermore, chimeric antigen receptor T cells, which target FAP-positive cells, have been recently reported to inhibit tumor growth by targeting tumor stroma [25, 26]. If FAP-positive fibroblasts play a role in stromal formation in the early stages of lung adenocarcinoma, as suggested in the present study, a therapeutic strategy that targets FAP-positive CAFs could be clinically effective for disturbing ECM formation, as reported previously [25, 26].

However, the current study has some limitations. First, this was a retrospective study performed at a single institution; therefore, the possibility of selection bias cannot be excluded. Second, since single-cell sequence analysis has recently identified several potential markers of CAFs other than αSMA and FAP [34], further analysis on the expression of these markers in early-stage lung adenocarcinoma is warranted. Third, we did not discuss the role of FAP as a proteolytic enzyme [35, 36], as we focused on the profibrotic role and stroma formation by FAP-positive fibroblasts in lung adenocarcinoma. As FAP-positive fibroblasts could be pivotal in the breakdown and turnover of the ECM via FAP's enzymatic activity [35, 36], further studies are warranted to elucidate whether FAP-positive fibroblasts could prompt invasiveness in adenocarcinoma by cleaving alveolar elastic fibers and disrupting the pre-existing alveolar structure.

Conclusions

Our findings show that the increase in αSMA expression relative to ISLR, which is a characteristic of CAFs, starts in the pre-existing alveolar septa of AAH lung tissues. Moreover, this change, including FAP expression, gradually progresses from AAH to IA through AIS. Our findings suggest that FAP-positive fibroblasts may contribute to tumor stroma formation in early-stage lung adenocarcinoma.

Supplementary Information The online version contains supplementary material available at https://doi.org/10.1007/s10147-024-02507-1.

Acknowledgements We would like to thank Editage (www.editage.com) for English language editing.

Author contributions All authors contributed to the study's conception and design. Toru Kimura, Takashi Akazawa, Yu Mizote, Harumi Nakamura, Miki Sakaue, Tomohiro Maniwa, Yasushi Shintani, Keiichiro Honma, Hideaki Tahara, and Jiro Okami carried out material preparation, and data collection and analysis. Toru Kimura wrote the first draft of the manuscript, and all authors commented on previous versions. All authors have read and approved the final manuscript.

Funding This research was supported by JSPS KAKENHI [Grant number JP19K09314].

Data availability All relevant data are presented in the manuscript.

Declarations

Conflict of interest The authors have declared that no competing interest exists.

Ethics approval and consent to participate This study was performed in line with the principles of the Declaration of Helsinki. The study was approved by the Institutional Review Board of the Osaka International Cancer Institute (June 12, 2019. Approval No. 19050). Written informed consent was obtained from all patients.

Consent for publication Not applicable.

References

1. Succony L, Rassl DM, Barker AP et al (2021) Adenocarcinoma spectrum lesions of the lung: detection, pathology and treatment strategies. Cancer Treat Rev 99:102237
2. World Health Organization (2021). Thoracic tumours, WHO classification of Tumours, 5th Edition, Volume 5. International Agency for Research on Cancer
3. Noguchi M (2010) Stepwise progression of pulmonary adenocarcinoma-clinical and molecular implications. Cancer Metastasis Rev 29:15–21
4. Travis WD, Brambilla E, Noguchi M et al (2011) International association for the study of lung cancer/american thoracic society/european respiratory society international multidisciplinary classification of lung adenocarcinoma. J Thorac Oncol 6:244–285
5. Kalluri R, Zeisberg M (2006) Fibroblasts in cancer. Nat Rev Cancer 6:392–401

6. Chen Y, McAndrews KM, Kalluri R (2021) Clinical and therapeutic relevance of cancer-associated fibroblasts. Nat Rev Clin Oncol 18:792–804
7. Maeda K, Enomoto A, Hara A et al (2016) Identification of Meflin as a potential marker for mesenchymal stromal cells. Sci Rep 6:22288
8. Kobayashi H, Gieniec KA, Wright JA (2021) The balance of stromal BMP signaling mediated by GREM1 and ISLR drives colorectal carcinogenesis. Gastroenterology 160:1224-1239.e30
9. Mizutani Y, Kobayashi H, Iida T et al (2019) Meflin-positive cancer-associated fibroblasts inhibit pancreatic carcinogenesis. Cancer Res 79:5367–5381
10. Miyai Y, Sugiyama D, Hase T et al (2022) Meflin-positive cancer-associated fibroblasts enhance tumor response to immune checkpoint blockade. Life Sci Alliance 5:e202101230
11. Augsten M (2014) Cancer-associated fibroblasts as another polarized cell type of the tumor microenvironment. Front Oncol 4:62
12. Avery D, Govindaraju P, Jacob M et al (2018) Extracellular matrix directs phenotypic heterogeneity of activated fibroblasts. Matrix Biol 67:90–106
13. Öhlund D, Handly-Santana A, Biffi G et al (2017) Distinct populations of inflammatory fibroblasts and myofibroblasts in pancreatic cancer. J Exp Med 214:579–596
14. Mathew S, Scanlan MJ, Mohan Raj BK et al (1995) The gene for fibroblast activation protein α (FAP), a putative cell surface-bound serine protease expressed in cancer stroma and wound healing, maps to chromosome band 2q23. Genomics 25:335–337
15. Kimura T, Monslow J, Klampatsa A et al (2019) Loss of cells expressing fibroblast activation protein has variable effects in models of TGF-β and chronic bleomycin-induced fibrosis. Am J Physiol Lung Cell Mol Physiol 317:L271–L282
16. Puré E, Blomberg R (2018) Pro-tumorigenic roles of fibroblast activation protein in cancer: back to the basics. Oncogene 37:4343–4357
17. Fitzgerald AA, Weiner LM (2020) The role of fibroblast activation protein in health and malignancy. Cancer Metastasis Rev 39:783–803
18. Moreno-Ruiz P, Corvigno S, te Grootenhuis NC et al (2021) Stromal FAP is an independent poor prognosis marker in non-small cell lung adenocarcinoma and associated with p53 mutation. Lung Cancer 155:10–19
19. Liao Y, Ni Y, He R et al (2013) Clinical implications of fibroblast activation protein-α in non-small cell lung cancer after curative resection: a new predictor for prognosis. J Cancer Res Clin Oncol 139:1523–1528
20. Min KW, Kim DH, Noh YK et al (2021) Cancer-associated fibroblasts are associated with poor prognosis in solid type of lung adenocarcinoma in a machine learning analysis. Sci Rep 11:16779
21. Pellinen T, Paavolainen L, Martín-Bernabé A et al (2023) Fibroblast subsets in non-small cell lung cancer: associations with survival, mutations, and immune features. J Natl Cancer Inst 115:71–82
22. Privé BM, Boussihmad MA, Timmermans B et al (2023) Fibroblast activation protein-targeted radionuclide therapy: background, opportunities, and challenges of first (pre)clinical studies. Eur J Nucl Med Mol Imaging 50:1906–1918
23. Windisch P, Zwahlen DR, Giesel FL et al (2021) Clinical results of fibroblast activation protein (FAP) specific PET for non-malignant indications: systematic review. EJNMMI Res 11:18
24. Giesel FL, Adeberg S, Syed M et al (2021) FAPI-74 PET/CT using either ^{18}F-AlF or cold-kit ^{68}Ga labeling: biodistribution, radiation dosimetry, and tumor delineation in lung cancer patients. J Nucl Med 62:201–207
25. Lo A, Wang LS, Scholler J et al (2015) Tumor-promoting desmoplasia is disrupted by depleting FAP-expressing stromal cells. Cancer Res 75:2800–2810
26. Wang LCS, Lo A, Scholler J et al (2014) Targeting fibroblast activation protein in tumor stroma with chimeric antigen receptor T cells can inhibit tumor growth and augment host immunity without severe toxicity. Cancer Immunol Res 2:154–166
27. Aghajanian H, Kimura T, Rurik JG et al (2019) Targeting cardiac fibrosis with engineered T cells. Nature 573:430–433
28. Kostrikov S, Johnsen KB, Braunstein TH et al (2021) Optical tissue clearing and machine learning can precisely characterize extravasation and blood vessel architecture in brain tumors. Commun Biol 4:815
29. Kanda Y (2013) Investigation of the freely available easy-to-use software "EZR" for medical statistics. Bone Marrow Transplant 48:452–458
30. Nurmik M, Ullmann P, Rodriguez F et al (2020) In search of definitions: cancer-associated fibroblasts and their markers. Int J Cancer 146:895–905
31. Sivakumar S, San Lucas FA, McDowell TL et al (2017) Genomic landscape of atypical adenomatous hyperplasia reveals divergent modes to lung adenocarcinoma. Cancer Res 77:6119–6130
32. Acharya PS, Zukas A, Chandan V et al (2006) Fibroblast activation protein: a serine protease expressed at the remodeling interface in idiopathic pulmonary fibrosis. Hum Pathol 37:352–360
33. Yotsukura M, Asamura H, Suzuki S et al (2020) Prognostic impact of cancer-associated active fibroblasts and invasive architectural patterns on early-stage lung adenocarcinoma. Lung Cancer 145:158–166
34. Lavie D, Ben-Shmuel A, Erez N et al (2022) Cancer-associated fibroblasts in the single-cell era. Nat Cancer 3:793–807
35. Fan MH, Zhu Q, Li HH et al (2016) Fibroblast activation protein (FAP) accelerates collagen degradation and clearance from lungs in mice. J Biol Chem 291:8070–8089
36. Zhang HE, Hamson EJ, Koczorowska MM et al (2019) Identification of novel natural substrates of fibroblast activation protein-alpha by differential degradomics and proteomics. Mol Cell Proteomics 18:65–85